17th Symposium IMEKO TC 4, 3rd Symposium IMEKO TC 19 and 15th IWADC Workshop
Instrumentation for the ICT Era
Sept. 8-10, 2010, Kosice, Slovakia

Digitally Controlled Current Source for Testing Circuit Breakers

Peter Višnyi, Jaroslav Dudrík, František Ďurovský

Technical University of Košice, Letná 9, Košice,
phone: +421 55 6022700, e-mail: peter.visnyi@tuke.sk

***Abstract*-**This document deals with a digitally controlled current source used for testing magnetic overcurrent releases of circuit breakers. The magnetic overcurrent releases of circuit breakers operate at much higher current than the nominal current. They are tested by a special current sources capable to provide currents up to hundreds or thousands of Amperes with an accuracy of a few percents. These current sources are designed for operation at very low voltage, typically less than 10 Volts (RMS) and at very short testing time (typicaly 100 ms) with long idle period. This document describes the digital current control that is very specific from the viewpoint of technical requirements as well as the used control method – digital current control without direct feedback.

I. Introduction

The current source used for testing magnetic overcurrent releases of circuit breakers represents a very interesting equipment from technical point of view. This current source has some specific properties:

- The current source must provide very high currents at very small voltages.
- The testing current is represented by a very accurate adjustable waveform with very short duration.

The current source described in this document was designed for generating adjustable sinusoidal current pulses of 50 Hz having duration of 100 ms (5 complete repeating periods) up to 2500 A (RMS). The operating voltage at the highest current does not exceed 10 V (RMS), from which an expressive part may be represented by the voltage drop of necessary inlet current path. The requirement of generating a high current at low voltage results in use of a conventional PWM power converter with a power transformer for stepping up the output current. The simplified power scheme of the current source including a power LC filter is shown in Fig. 1.

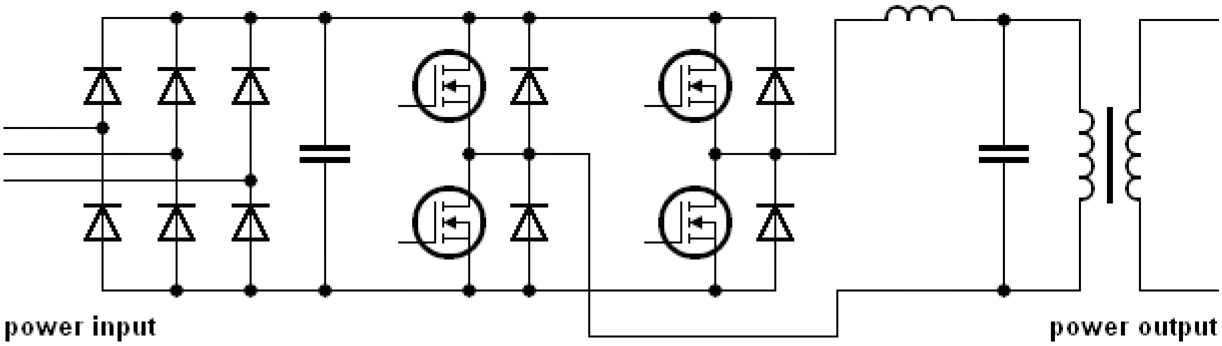

Figure 1. Simplified power scheme of the current source

The power converter contains a DSP for calculating and generating a proper PWM control signals for the power transistors. The external LC filter is a substantial part of the power scheme. It removes from the output voltage of the PWM converter the high frequency components and makes the output voltage and current smooth. On the other hand, the LC filter makes the current control more difficult because it increases the complexity of the controlled system.

The particularity of the current control consists in the following reasons. The typical turn-off time of magnetic overcurrent releases is less than a sinusoidal half period (10 ms) which is much less than the capability of the current source (100 ms). At such short duration of the testing current it is very important that the current waveform must have the prescribed shape from the very beginning to the end with high accuracy. This requirement cannot be fulfilled by conventional current control where the steady-state with zero control error is preceded by a transient state with high control error. At conventional current control the control transient states might have duration larger than one sinusoidal period that is absolutely inadmissible.

II. Principle of current control

It is evident that the most difficult technical task consists not in generating an extremely high current but in obtaining the accurate prescribed current waveform without any transient state. The current control method used for the described current source is specific by the fact that it does not use direct feedback. It is based on having a very accurate mathematical model of the whole current control system and calculating the PWM control value without need for current feedback information. The accuracy of such control depends on the accuracy of the mathematical model used for calculation of the PWM control value. Therefore the mathematical model of the PWM converter incudes its non-linearity described by a table in the fixed memory of the microcontroller, as well as the mathematical model of the filtering inductance. Aditionally, the accurate capacitance of the LC filter must be known. As to the transformer, it has a negligible magnetizing current at working voltage and so it is described by one parameter only (transformation ratio). The only parameters of the system that cannot be stored in the fixed memory are the parameters of the load impedance because they inlude the resistance and inductance of the circuit breaker to be connected to the testing terminals. Therefore the overall load resistance and inductance is measured before the test begins and these parameters are included in the mathematical model of the system. The measurement of the load parameters is performed at very low current in steady state at frequency of 50 Hz. Using correct information of the load resistance, the resulting current from the very beginning has a good accuracy, correct shape and a small control error.

III. Principle of PWM pulses generation

The control PWM pulses for the transistors of the power converter are generated by the control DSP. The principle of pulses generation is evident from Fig. 2 showing the waveforms of the internal digital variables of the DSP as well as the waveforms of the resulting PWM pulses. The symmetrical sawtooth signal represented by the black line is the the digital time base of the PWM module generated by the internal hardware of the DSP. The lower peak of the time base signal has the zero value and the upper peak has the value **T** representing the half period of the time base expressed as number of clock periods of the PWM module. The blue and red lines cutting the time base represent two digital parameters (variables) $\mathbf{t_a}$, $\mathbf{t_b}$. It is evident from Fig. 2 how these parameters determine the resulting waveforms of the PWM pulses. The edges of the PWM pulses correspond to the instants where the sawtooth signal value is equal to the PWM parameters $\mathbf{t_a}$, $\mathbf{t_b}$.

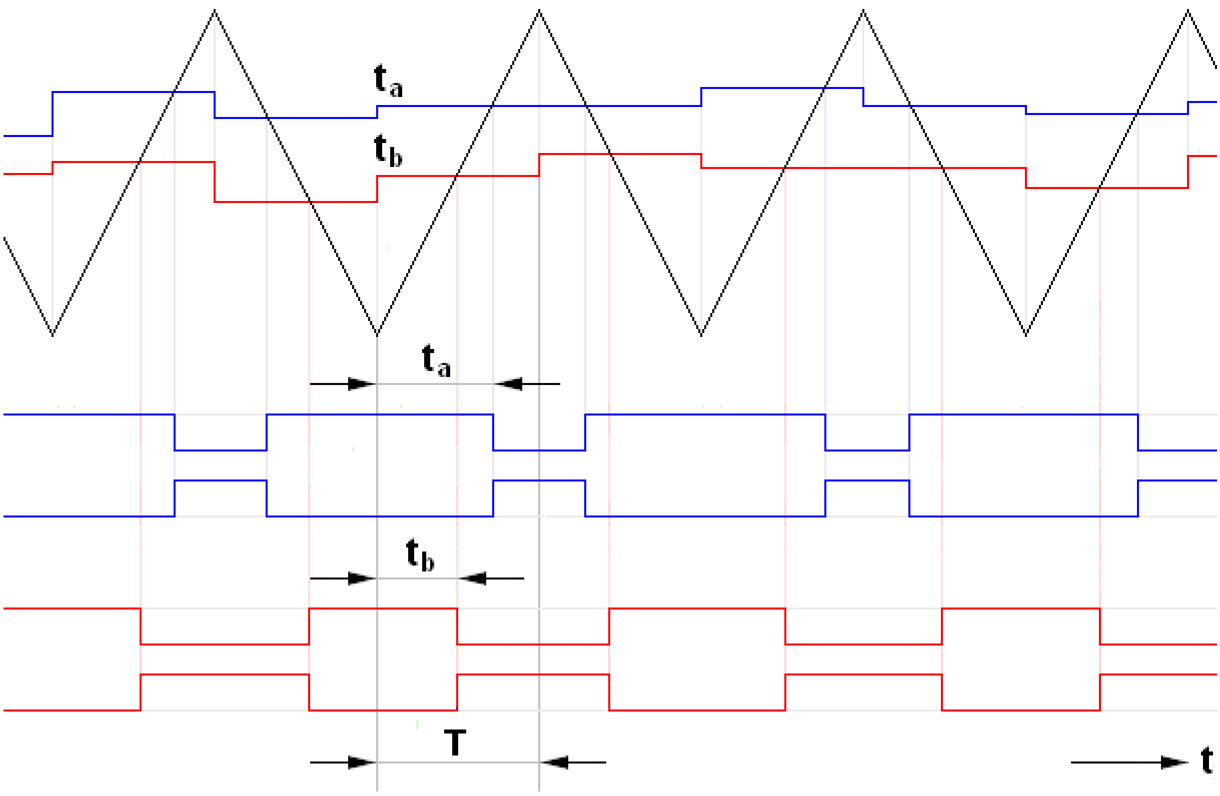

Figure 2. Principle of PWM pulses generation

The complementary pairs of PWM pulses are generated with a small dead-band delay that is not visible in Fig. 2. New values of the PWM parameters $\mathbf{t}_a$, $\mathbf{t}_b$ are calculated by the DSP program for current control during each half period $\mathbf{T}$ (between two subsequent peaks of the time base) and are updated by the hardware at the beginning of the next half period (as evident from Fig. 2). The values of the PWM parameters $\mathbf{t}_a$, $\mathbf{t}_b$ fall in the interval from zero to $\mathbf{T}$. The time $\mathbf{T}$ represents one cycle of the DSP program as well as one sampling period for all variables in the control algorithm. As the result of the PWM control pulses generation, power PWM pulses are generated at the output terminals of the PWM converter (input terminals of the LC filter) and a sinusoidal average voltage of 50 Hz frequency is obtained at the output terminals of the LC filter. The time behaviour of the power PWM pulses depends directly on the time behaviour of the PWM parameters $\mathbf{t}_a$, $\mathbf{t}_b$ generated by the control program. The theoretical average value of the power PWM voltage at no-load condition is expressed by

$$\mathbf{u}_{x0} = \mathbf{u}_{DC}\,(\mathbf{t}_a - \mathbf{t}_b) / \mathbf{T} \qquad (1)$$

where $\mathbf{u}_{DC}$ is the DC link voltage. Practically the resulting average value includes a voltage drop that has a non-linear dependence on the load current. In this application the parameters $\mathbf{t}_a$, $\mathbf{t}_b$ are calculated using the equations

$$\mathbf{t}_a = \mathbf{T}/2 + \mathbf{t}_x \qquad (2)$$

$$\mathbf{t}_b = \mathbf{T}/2 - \mathbf{t}_x \qquad (3)$$

where $\mathbf{t}_x$ is the common control variable that determines the voltage $\mathbf{u}_{x0}$ according to the equation

$$\mathbf{u}_{x0} = 2\,\mathbf{u}_{DC}\,\mathbf{t}_x / \mathbf{T} \qquad (4)$$

The value $\mathbf{t}_x$ oscillates theoretically in the interval (-$\mathbf{T}$/2, $\mathbf{T}$/2), practically the interval is slightly reduced due to a small dead-band delay of the PWM pulses. Such PWM control mode is known as unipolar control mode. At this control mode the output power PWM pulses have unipolar character and their frequency is equal to 1/$\mathbf{T}$. The polarity of the power PWM pulses depends only on the sign of the variable $\mathbf{t}_x$.

IV. Discontinuous mathematical model of the control system

All variables calculated by the DSP including PWM parameters $\mathbf{t}_a$, $\mathbf{t}_b$ represent discrete variables (progressions of samples with sampling period $\mathbf{T}$) and can be matematically expressed as functions of integer variable $\mathbf{n}$ representing the time. Therefore the mathematical model of the control system (consisting of the PWM converter, LC filter, transformer and load impedance) to be used for current control is discontinuous, i.e described by equations of discrete variables. The mathematical model of the system is described by a system of discrete equations describing the individual parts of the system. The equations are obtained from the equivalent block diagram of the control system (Fig. 3). In this diagram the resistanc R and inductance L represent the transformed value of the real load impedance at the output of the transformer. That is why the transformer is not necessery in the equivalent block diagram. The parameter R includes the resistance of the transformer and the parameter L includes the leakage inductances of the transformer. The capacitance C and the inductance L_x represent the LC filter. In this equivalent block diagram there are two non-linear elements described by non-linear equations. The first non-linear element is the PWM converter with the non linear dependence of the ouptut voltage drop on the load current. For practical reasons the voltage drop of the filtering inductor's resistance was included in the voltage drop of the PWM converter. That is why this block diagram does not contain the resistance of the filtering inductor and the inductance L_x represents a lossless nonlinear inductor – the second non-linear element of the block diagram.

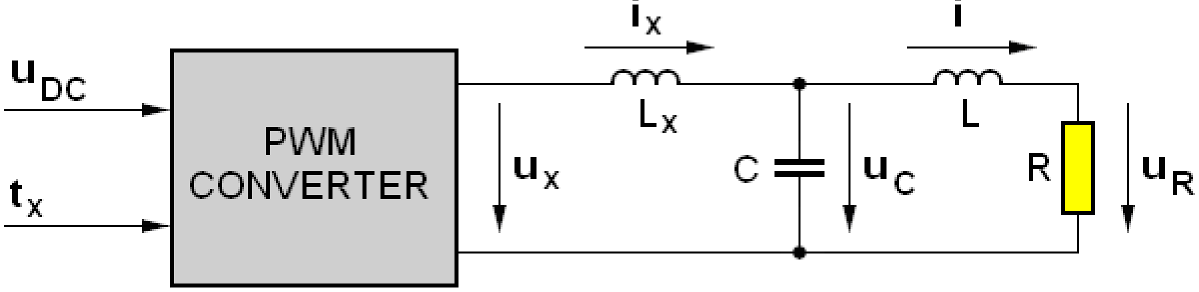

Figure 3. Equivalent block diagram of the control system

It has non-linear dependence of the voltage integral on the current (magnetization curve). Both the non-linear elements are described by non-linear functions obtained by measurement and written to the DSP memory. The equivalent block diagram contains several electrical variables: $\mathbf{u}_{DC}$ - DC link voltage of the PWM converter, $\mathbf{u}_x$ - output voltage of the PWM converter, $\mathbf{u}_{x0}$ - the output voltage of the PWM converter at zero load current, $\mathbf{u}_C$ – voltage of the filtering capacitor C, $\mathbf{u}_R$ – voltage of the load resistor R, $\mathbf{i}_x$ – load current of the PWM converter, $\mathbf{i}$ – output current, $\mathbf{u}_L$ – voltage of the filtering inductor L. In order to describe the equivalent block diagram by discrete equations and to derive a current control algorithm it is useful to define the following discrete variables :

- $\mathbf{t}_x(\mathbf{n})$ is the PWM parameter for the time interval between $\mathbf{t} = \mathbf{n}.\mathbf{T}$ and $\mathbf{t} = (\mathbf{n}+1).\mathbf{T}$
- $\mathbf{u}_{DC}(\mathbf{n})$ is the average voltage $\mathbf{u}_{DC}$ for the time interval between $\mathbf{t} = \mathbf{n}.\mathbf{T}$ and $\mathbf{t} = (\mathbf{n}+1).\mathbf{T}$
- $\mathbf{u}_x(\mathbf{n})$ is the average voltage $\mathbf{u}_x$ for the time interval between $\mathbf{t} = \mathbf{n}.\mathbf{T}$ and $\mathbf{t} = (\mathbf{n}+1).\mathbf{T}$
- $\mathbf{u}_{x0}(\mathbf{n})$ is the average voltage $\mathbf{u}_{x0}$ for the time interval between $\mathbf{t} = \mathbf{n}.\mathbf{T}$ and $\mathbf{t} = (\mathbf{n}+1).\mathbf{T}$
- $\mathbf{u}_C(\mathbf{n})$ is the average voltage $\mathbf{u}_C$ for the time interval between $\mathbf{t} = \mathbf{n}.\mathbf{T}$ and $\mathbf{t} = (\mathbf{n}+1).\mathbf{T}$
- $\mathbf{u}_R(\mathbf{n})$ is the average voltage $\mathbf{u}_R$ for the time interval between $\mathbf{t} = \mathbf{n}.\mathbf{T}$ and $\mathbf{t} = (\mathbf{n}+1).\mathbf{T}$
- $\mathbf{u}_L(\mathbf{n})$ is the average voltage $\mathbf{u}_L$ for the time interval between $\mathbf{t} = \mathbf{n}.\mathbf{T}$ and $\mathbf{t} = (\mathbf{n}+1).\mathbf{T}$
- $\mathbf{u}_{Lx}(\mathbf{n})$ is the average voltage $\mathbf{u}_{Lx}$ for the time interval between $\mathbf{t} = \mathbf{n}.\mathbf{T}$ and $\mathbf{t} = (\mathbf{n}+1).\mathbf{T}$
- $\mathbf{i}_x(\mathbf{n})$ is the instantaneous value $\mathbf{i}_x$ in the time instant $\mathbf{t} = \mathbf{n}.\mathbf{T}$
- $\mathbf{i}(\mathbf{n})$ is the instantaneous value $\mathbf{i}$ in the time instant $\mathbf{t} = \mathbf{n}.\mathbf{T}$

The discontinuous mathematical model of the control system is obtained by describing the individual parts of the equivalent block diagram by discrete equations. From equation (4) we obtain the discrete output voltage of the PWM converter at zero load current

$$\mathbf{u}_{x0}(\mathbf{n}) = 2\, \mathbf{u}_{DC}(\mathbf{n})\, \mathbf{t}_x(\mathbf{n}) / \mathbf{T} \tag{5}$$

At variable load current $\mathbf{i}_x$ the output voltage of the PWM converter is lowered by the voltage drop of the PWM converter having a non-linear dependence on the load current $\mathbf{i}_x$, and by the voltage drop of the resistance R_0 of the filtering inductor**.** The voltage drop to be subracted from $\mathbf{u}_{x0}(\mathbf{n})$ is related to the time interval between $\mathbf{t} = \mathbf{n}.\mathbf{T}$ and $\mathbf{t} = (\mathbf{n}+1).\mathbf{T}$ and therefore it is expressed as dependence on the average current

$$\mathbf{i}_{xav}(\mathbf{n}) = [\mathbf{i}_x(\mathbf{n}) + \mathbf{i}_x(\mathbf{n}+1)] / 2 \tag{6}$$

The proposed non-linear description of the PWM converter is expressed by

$$\mathbf{u}_x(\mathbf{n}) = \mathbf{u}_{x0}(\mathbf{n}) - F_1[\mathbf{i}_{xav}(\mathbf{n}) / \mathbf{u}_{DC}(\mathbf{n})] - R_0\, \mathbf{i}_{xav}(\mathbf{n}) \tag{7}$$

where F_1 is a non-linear function representing the voltage drop of the PWM converter at real load current, R_0 is the resistance of the filtering inductor. The equation (7) does not describe the PWM converter exactly, however having got a proper non-linear function F_1 the equation (7) describes the behaviour of the PWM converter with very good accuracy. The values of the voltage drop are relatively small, however cannot be neglected and must be calculated by equation (7) in order to maintain the mathematical model of the PWM converter at sufficient accuracy. The mathematical description of the inductor L_x is based on idea of a lossless non-linear inductor described by equation

$$\mathbf{u}_{Lx}(\mathbf{n}) = F_2[\mathbf{i}_x(\mathbf{n}+1)] - F_2[\mathbf{i}_x(\mathbf{n})] \tag{8}$$

The non-linear function $F_2(\mathbf{i})$ is defined as the average voltage necessary for increasing the current of the inductor from zero to value $\mathbf{i}$ in the time interval $\mathbf{T}$. This dependence is equivalent to the magnetizing curve of the core neglecting the hysteresis. The non-linear functions F_1 and F_2 are obtained by special measurements and their good validity can be proved practically. The discontinuous mathematical model of the linear passive elements C, L, R is expressed by equations

$$\mathbf{i}_C(\mathbf{n}) = C\, [\mathbf{u}_C(\mathbf{n}) - \mathbf{u}_C(\mathbf{n}-1)] / \mathbf{T} \tag{9}$$

$$\mathbf{u}_L(\mathbf{n}) = L\, [\mathbf{i}(\mathbf{n}+1) - \mathbf{i}(\mathbf{n})] / \mathbf{T} \tag{10}$$

$$\mathbf{u}_R(\mathbf{n}) = R\, [\mathbf{i}(\mathbf{n}) + \mathbf{i}(\mathbf{n}+1)] / 2 \tag{11}$$

The complete mathematical description of the block diagram in Fig. 3 should include the equations describing the connection of the individual elements. They can be obtained by applying the Kirchhoff's laws to this scheme.

The presented discontinuous mathematical model of the control system is not perfect. However, it is sufficiently accurate and at the same time sufficiently simple. All the parameters and non-linearities in the mathematical model except the parameters R, L are obtained by precise measurement at the stage of design and included in the control program. The parameters R, L represent the properties of the tested circuit breaker. They may be different for different circuit breakers. Therefore the overall impedance parameters are measured automatically before the test begins. The measurement is made at the rated current of the circuit breaker that is very small in comparison with the testing currents and has no effect on the test result.

V. Mathematical description of the current control

In general, the waveworm of the required (reference) output current $\mathbf{i}(\mathbf{n})$ must be given by a look-up table in the DSP memory. The concrete required current waveform consists of five 50 Hz sinusoidal periods (with resulting duration of 100 ms) and it is stored in the memory as a progression of discrete current samples with sampling period $\mathbf{T}$. The waveform of the DC link voltage $u_{DC}(\mathbf{n})$ is obtained in real time by measurement also as a progression of voltage samples. Using the proposed mathematical model, from these input waveforms it is possible to perform calculation of the PWM control variable $\mathbf{t}_x$ as well as control variables $\mathbf{t}_a$, $\mathbf{t}_b$ as discrete progressions. The following calculation algorithm is performed in the time interval between $\mathbf{t} = (\mathbf{n}-2).\mathbf{T}$ and $\mathbf{t} = (\mathbf{n}-1).\mathbf{T}$. As the result it provides the PWM control values $\mathbf{t}_a(\mathbf{n}-1)$ and $\mathbf{t}_b(\mathbf{n}-1)$, using the reference current samples $\mathbf{i}(\mathbf{n})$, $\mathbf{i}(\mathbf{n}+1)$. That means the PWM control values must be calculated with advance of three steps with respect to the reference current samples. This is implication of the fact that the reactance elements of the system as well as the PWM system represent an inherent delay elements in the control system.
The calculation algorithm begins with calculation of $\mathbf{u}_C(\mathbf{n})$ using equation

$$\mathbf{u}_C(\mathbf{n}) = R\,[\mathbf{i}(\mathbf{n}) + \mathbf{i}(\mathbf{n}+1)] / 2 + L\,[\mathbf{i}(\mathbf{n}+1) - \mathbf{i}(\mathbf{n})] / \mathbf{T} \tag{12}$$

The equation results from equations (10), (11) and the 2nd Kirchhoff's law applied to $\mathbf{u}_C$, $\mathbf{u}_L$, $\mathbf{u}_R$ (see Fig. 3). The value $\mathbf{i}_C(\mathbf{n})$ is calculated using equation

$$\mathbf{i}_C(\mathbf{n}) = C\,[\mathbf{u}_C(\mathbf{n}) - \mathbf{u}_C(\mathbf{n}-1)] / \mathbf{T} \tag{9}$$

where the value $\mathbf{u}_C(\mathbf{n}-1)$ represents the value $\mathbf{u}_C(\mathbf{n})$ obtained in the previous step by equation (12). Using the 1st Kirchhoff's law the value $\mathbf{i}_x(\mathbf{n})$ is obtained by

$$\mathbf{i}_x(\mathbf{n}) = \mathbf{i}_C(\mathbf{n}) + \mathbf{i}(\mathbf{n}) \tag{13}$$

The value $\mathbf{u}_{Lx}(\mathbf{n}-1)$ is calculated by the equation (8) applied to the previous step by equation

$$\mathbf{u}_{Lx}(\mathbf{n}-1) = F_2[\mathbf{i}_x(\mathbf{n})] - F_2[\mathbf{i}_x(\mathbf{n}-1)] \tag{14}$$

where the value $\mathbf{i}_x(\mathbf{n}-1)$ represents the value $\mathbf{i}_x(\mathbf{n})$ obtained in the previous step by equation (13). The output voltage sample $\mathbf{u}_x(\mathbf{n}-1)$ is obtained from $\mathbf{u}_{Lx}(\mathbf{n}-1)$ and $\mathbf{u}_C(\mathbf{n}-1)$ using the 2nd Kirchhoff's law by equation

$$\mathbf{u}_x(\mathbf{n}-1) = \mathbf{u}_C(\mathbf{n}-1) + \mathbf{u}_L(\mathbf{n}-1) \tag{15}$$

In order to obtain the value $\mathbf{u}_{x0}(\mathbf{n}-1)$ the voltage drops must be subtracted from $\mathbf{u}_x(\mathbf{n}-1)$ using equations

$$\mathbf{i}_{xav}(\mathbf{n}-1) = [\mathbf{i}_x(\mathbf{n}-1) + \mathbf{i}_x(\mathbf{n})] / 2 \tag{16}$$

$$\mathbf{u}_{x0}(\mathbf{n}-1) = \mathbf{u}_x(\mathbf{n}-1) + F_I\,[\mathbf{i}_{xav}(\mathbf{n}-1) / \mathbf{u}_{DC}(\mathbf{n}-1)] + R_0\,\mathbf{i}_{xav}(\mathbf{n}-1) \tag{17}$$

derived from equations (6) and (7). The PWM parameters $\mathbf{t}_a(\mathbf{n}-1)$, $\mathbf{t}_b(\mathbf{n}-1)$ are obtained by equations

$$\mathbf{t}_x(\mathbf{n}-1) = \mathbf{T}\,\mathbf{u}_{x0}(\mathbf{n}-1) / (2\,\mathbf{u}_{DC}(\mathbf{n}-1)) \tag{18}$$

$$\mathbf{t}_a(\mathbf{n}-1) = \mathbf{T}/2 + \mathbf{t}_x(\mathbf{n}-1) \tag{19}$$

$$\mathbf{t}_b(\mathbf{n}-1) = \mathbf{T}/2 - \mathbf{t}_x(\mathbf{n}-1) \tag{20}$$

derived from equations (2), (3), (4).

VI. Design of the look-up table of the required current

The look-up table of the required current contains the scaled waveform of the required current consisting of five sine cycles (Fig. 4).

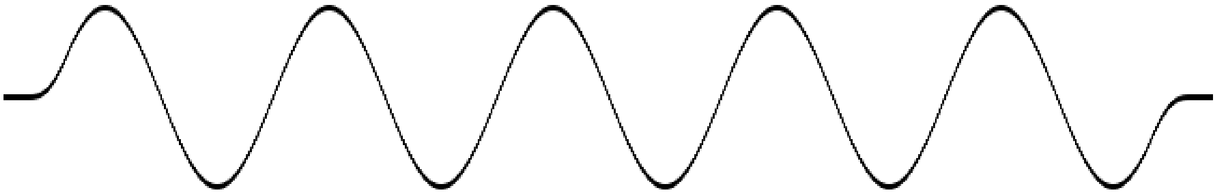

Fig.4. Waveform of the required current

From the figure it is evident that the waveform has no sharp transitions at the beginning and at the end. In fact, at the beginning and at the end the sine function is replaced by polynomic functions of the third order so that the waveform as well as its first and second time derivation are continuous. The reason is the following. The reactances of the system do not allow the output current and its derivations to change discontinuously. If the look-up table would not respect this limitations the current control calculations should result in such high peaks of the voltage $\mathbf{u}_x(\mathbf{n})$ that are beyond the inherent working range and cannot be produced by the converter. As a consequence the calculated value $\mathbf{t}_x$ should be limited to its maximum possible value ± T/2. This limitation should cause unwanted deformation (resonant oscillations) of the output current at the beginning and at the end of the current waveform. It is better to respect the existing limitations and to design the reference current waveform according to Fig. 4 and to prevent unwanted deformation. By using such reference current waveform the necessary voltage peaks at the beginning and at the end are not too high and no limitation of the PWM parameters is necessary, so that the real current waveform corresponds with the designed waveform (Fig. 4).

VII. Conclusions

The presented current control method was sucessfully applied in a prototype of a testing equipment for circuit brakers. The used DSP was TMS320F2406A, the PWM clock frequency was 40 MHz. The chosen switching frequency of the PWM converter was 10 kHz, the sampling period **T** was 50 μs. Thanks to getting a very precise mathematic model including non-linear function tables the current waveform generated without any current feedback had very small deformation (hardly visible by oscilloscope) and the error of the amplitude was not larger than 5 %. The inacuracies of the current control were caused by the fact that the non-linear mathematical model of the converter is not absolutely correct. Some compensation (elimination) of the amplitude error might be possible if necessary. The compensation should be based on known amplitude error measured at various values of the current amplitude and load resistance. The experiments with short time current pulses proved that the prescribed current shape was kept from the beginning to the end without any transient state. In order to prove the current control method using the non-linear mathematic model, some experiments were made using linear functions replacing the non-linearities. They resulted in a very deformed current, unlike using the non-linear mathematical model with negligible resulting current deformation.

The automatic measurement of the parameters R, L is based on a short recorded history of the progressions $\mathbf{u}_\mathbf{x}$(n), **i**(n) and the described mathematical model of the current control circuit. The detailed description of the measurement is not the subject of this paper. It was proved that measuring the parameters R, L not only before the test but also during the test itself may be useful because due to high instantaneous power losses of the load (current breaker) its temperature increases during miliseconds that results in changes in the values R, L during the test. Measuring parameters R, L before the test (in cold state) provides only the initial values of R, L.

Measuring the non-linear characteristics of the converter and the filtering inductor is based on a recorded history of the progressions $\mathbf{t}_\mathbf{x}$(n), $\mathbf{u}_{\mathbf{DC}}$(n), **i**(n) and the described mathematical model of the current control circuit. The detailed mathematical description of such measurement is not the subject of this paper.

Fig. 5 shows the typical current waveform (i) obtained by current control along with the voltage waveform (u_C). Fig. 5a shows a detail of one sinusoidal period of the current and voltage, Fig. 5b shows the same situation at different time base enabling to see the whole current waveform of duration 100 ms. It is evident that due to a small inductive component of the load impedance the phase shift between the current and the voltage is visible. In addition, it is evident, that at correct waveform **i** of the current at the beginning, the voltage $\mathbf{u}_C$ must have at the beginning a jump. From Fig. 5b it is evident, that due to the phase shift at the end of the current waveform another jump of voltage is needed. Due to soft beginning and ending of the reference current the jumps of the voltage need not to be very sharp and can be generated accurately despite of the effect of the LC filter.

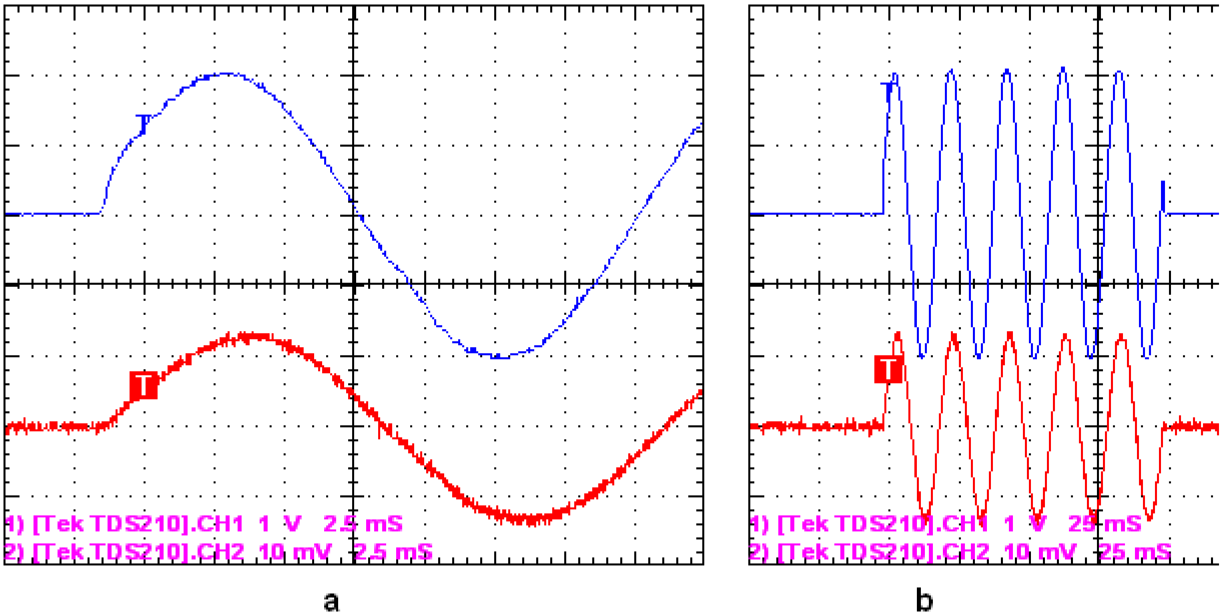

Fig.5. The real current **i** (red) and voltage $\mathbf{u}_C$ (blue) measured by oscilloscope

Acknowledgement

This work was supported by Slovak Research and Development Agency under projects APVT-20-P03105 and APVV-0095-07.

References

[1] A. M. Stankovic, D.J. Perreault, K. Sato, “Discrete-time current control of voltage-fed three-phase PWM inverters”, *IEEE Transactions on Power Electronics*, vol. 14, No. 2, 1996

[2] Lennart Harnefors, Hans-Peter Nee, “Model-based current control of AC machines using the internal model control method”, *IEEE Transactions on Industry Applications*, vol. 34, No. 1, January/February 1998

[3] Hasan Komurcugil, Osman Kukrer, “A novel current control method for three-phase PWM AC/DC voltage source converters”, *IEEE Transactions on Industrial Electronics*, vol. 46, No. 3, June 1999

[4] Jose Rodriguez, Jorge Pontt, Cesar A.Silvia, Pablo Corea, Pablo Lezana, “Predictive current control of a voltage source inverter”, *IEEE Transactions on Industrial Electronics*, vol. 14, No. 1, February 2007

[5] D. G. Holmes, D. A. Martin, “Implementaion of a direct digital predictive current controller for single and three phase voltage source inverters”, *IEEE-IAS Annual Meeting*, San Diego, 1996

[6] O. Kurker, “Discrete-time current control of voltage-fed three phase PWM inverters”, *IEEE Transactions on Power Electronics*, vol. 11, 1996

[7] H. Le-Huy, K. Slimani, P. Viarouge, Analysis and implementation of a real-time predictive current controller for permanent-magnet synchronous servo drives”, *IEEE Transactions on Industrial Electronics*, vol. 41, 1994